Adapting Antibody–Invertase Fusion Protein Immunoassays to Multiwell Plates for Infectious Disease Antibody Quantification

Elysse Ornelas-Gatdula[1], Xinran An[2,3], Jamie B. Spangler[2,3,4,5,6,7,8,9], and Netzahualcóyotl Arroyo-Currás[1,10,11,*]

[1] Chemistry-Biology Interface Program, Zanvyl Krieger School of Arts & Sciences, Johns Hopkins University, Baltimore, MD 21218, United States

[2] Department of Chemical and Biomolecular Engineering, Johns Hopkins University, Baltimore, MD 21205, United States

[3] Translational Tissue Engineering Center, Johns Hopkins University School of Medicine, Baltimore, MD 21205, United States

[4] Department of Biomedical Engineering, Johns Hopkins University School of Medicine, Baltimore, MD 21205, United States

[5] Bloomberg-Kimmel Institute for Cancer Immunotherapy, Johns Hopkins University, Baltimore, MD 21205, United States

[6] Sidney Kimmel Comprehensive Cancer Center, Johns Hopkins University, Baltimore, MD 21205, United States

[7] Department of Oncology, Johns Hopkins University School of Medicine, Baltimore, MD 21205, United States

[8] Department of Ophthalmology, Johns Hopkins University School of Medicine, Baltimore, MD 21205, United States

[9] Department of Molecular Microbiology & Immunology, Johns Hopkins University Bloomberg School of Public Health, Baltimore, MD 21205, United States

[10] Department of Pharmacology and Molecular Sciences, Johns Hopkins University School of Medicine, Baltimore, MD 21205, United States

[11] *Current address:* Department of Chemistry, University of North Carolina at Chapel Hill, Chapel Hill, NC 27514, United States

* Correspondence to:

Netz Arroyo, Ph.D.
narroyo@unc.edu

Table of Contents

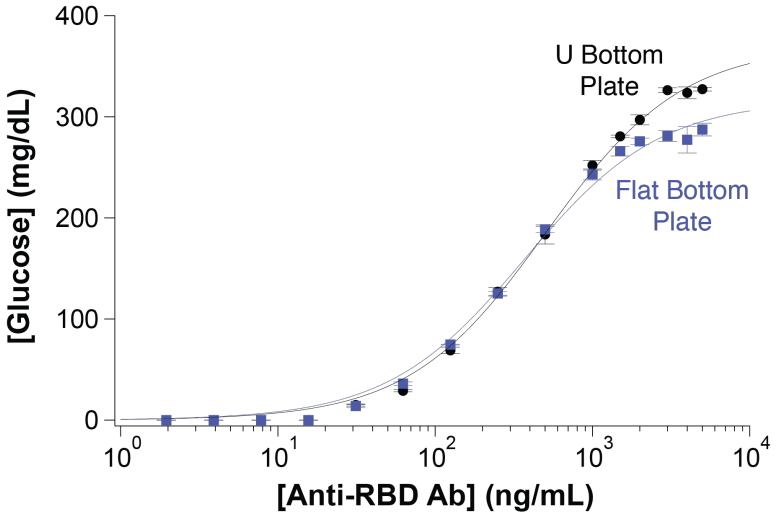

Figure S1. Signal output measured via glucose concentration is affected by the plate well geometry. Utilizing a round bottom plate increases the surface area on which antigens can passively adsorb when compared to a flat bottom plate.[1] Maximum glucose concentration under the same incubation conditions for a flat bottom plate and a round bottom plate are 317 ± 6 mg/dL and 371 ± 5 mg/dL, respectively.

Note on Instrument Costs

The primary cost drivers for high-end spectrophotometers include specialized optical components, precision mechanical engineering, and proprietary software, all of which contribute to higher manufacturing costs, especially given the relatively low production volumes typical of scientific instrumentation. While diode-based spectrometers are indeed more economical than traditional systems due to their use of solid-state components and simplified designs, they remain significantly more expensive than consumer-grade glucometers. For example, entry-level diode-array spectrometers are available for approximately $1,600, with more advanced systems costing tens of thousands of dollars. In contrast, basic glucometers are widely available for under $100, benefiting from mass production and economies of scale in the consumer health market.

Table S1. Commercially available photodiode-based spectrometers and their cost. This table is based on an internet search completed on 10/05/2025.

Plate Reader	Cost	Reference
Byonoy Absorbance 96	$3,850 – $5,329	DOI:10.1016/j.isci.2024.111080
Bio-Techne SimpleReader	$4,750	No publication found
BioLegend Mini ELISA Plate Reader	$4,395	DOI:10.1002/ppap.202400104

Table S2. Lateral cost analysis of diode-based spectrometers vs glucometers. Based on online search completed on 10/05/2025.

Device Type	Price	Technology	Market Volume
Diode-based Spectrometer	Starting around $1,600; advanced systems can cost tens of thousands	Uses advanced optics and solid-state sensors to measure light absorption	Niche scientific and industrial markets; lower production volumes
Glucometer	Typically under $100; recurring cost for test strips	Uses electrochemical detection via disposable test strips	Mass-produced for consumer health; high production volumes reduce cost

Table S3. Concentrations of LC15 used in the different assay formats. The MW of LC15 is 265,340 Da. The strip format requires 5-fold the concentration of the detection antibody when compared to the multiwell plate format.

Method	µM	µg/mL
Strips	0.1	26.5
Plate	0.02	5.3

Table S4. LC15 incubation time affects glucose output. First, we performed a One-Way ANOVA to determine if we could pool the data for [anti-RBD Ab] > 2000 ng/mL within each LC15 incubation time data set. For each incubation time, there was no significant difference in glucose output when [anti-RBD Ab] > 2000 ng/mL, indicating that RBD to anti-RBD Ab binding is fully saturated ($p_{15min} = 0.362$, $p_{30min} = 0.109$, $p_{60min} = 0.064$). Therefore, we chose to pool the data at these higher concentrations for each time point for further analysis. A One-Way ANOVA indicated that the maximum glucose output at saturation ([anti-RBD Ab] ≥ 2000 ng/mL, n = 12) is significantly different for the three incubation times ($p <<< 0.01$). Independent t-tests were then performed with a Bonferroni Correction ($\alpha = 0.05/3 = 0.0167$) and while the maximum glucose output at saturation for the 15-min and 30-min long incubations times were not significantly different from each other ($p = 0.643$), the maximum glucose output for the 60 min-long LC15 incubation is significantly different from the 15 min-long and 30-min long incubation times ($p <<< 0.01$ and $p <<< 0.01$, respectively).

LC15 Incubation Time (min)	**Max (mg/dL)**	**EC_{50} (ng/mL)**
15	370 ± 11	505 ± 56
30	363 ± 6	381 ± 28
60	396 ± 8	387 ± 31

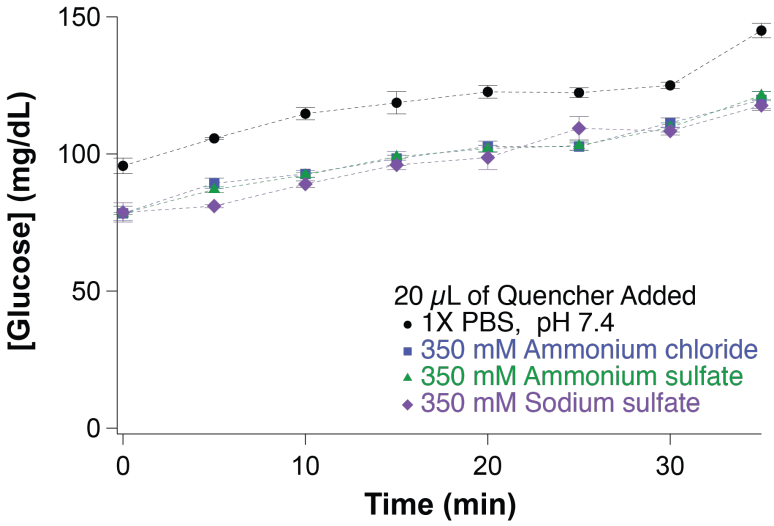

Figure S2. Invertase cannot be effectively quenched with an inhibitor. Solutions of known inhibitors: 350 mM ammonium chloride, 350 mM ammonium sulfate, and 350 mM sodium sulfate were prepared in 1X PBS, *p*H 7.4. As this was a time dependent assay, protein concentrations were kept constant with RBD = 0.1 µM, anti-RBD Ab = 500 ng/mL, and LC 15 = 0.02 µM. After incubating with sucrose for one hour, 20 µL of control solution (1X PBS, *p*H 7.4) or salt inhibitor (n = 3 for each time point) was added to assigned wells and the plate was shaken on a ThermoMixer at 25 °C, 500 rpm for 1 min prior to the glucose measurement step. Each of the proposed salt inhibitors failed to inhibit the conversion of sucrose to glucose over the duration required to manually read the plate. At 0 min, we expected that the control and the salt inhibitors to have the same initial glucose reading. However, we see a decrease in the glucose measurement for upon the addition of any of the salt inhibitor solutions, suggesting they are also having some inhibitory effect on glucose oxidase.

Table S5. The Hill equation derived for each of the drift-free curves when anti-RBD Ab is spiked in blocking buffer.

Row	Max (mg/dL)	EC_{50} (ng/mL)	Equation
A	312 ± 12	462 ± 66	x = 462/[(312/y)-1]
B	338 ± 12	478 ± 62	x = 478/[(338/y)-1]
C	345 ± 10	448 ± 48	x = 448/[(345/y)-1]
D	364 ± 10	420 ± 44	x = 420/[(364/y)-1]
E	372 ± 11	379 ± 41	x = 379/[(372/y)-1]
F	387 ± 10	350 ± 36	x = 350/[(387/y)-1]
G	387 ± 11	341 ± 36	x = 341/[(387/y)-1]
H	386 ± 12	292 ± 36	x = 292/[(386/y)-1]

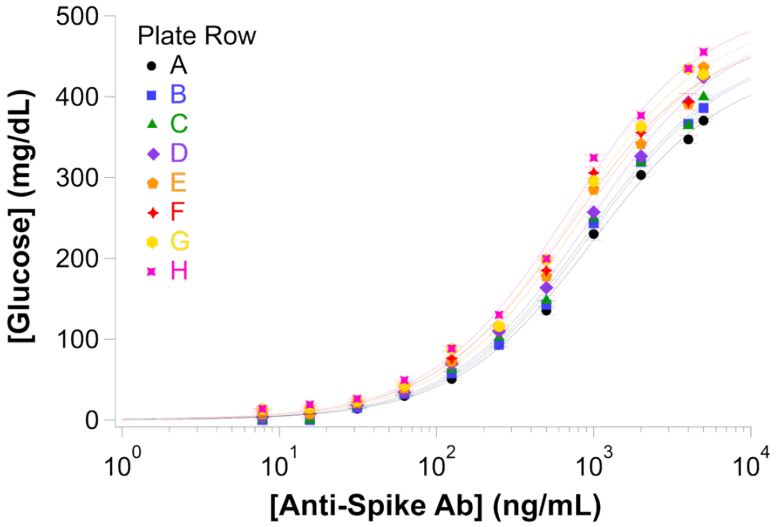

Figure S3. Dose-response curve for 20Ab spiked into 1% human plasma. The anti-Spike Ab is a 1:1:1 mixture of commercially produced RBD (Abcam PN: ab273073), S1 (Novus Biologicals PN: NBP3-07956), and NTD (ACROBiosystems PN: SPD-S164) monoclonal antibodies. 20% human plasma was prepared by diluting pooled donor plasma previously confirmed negative for SARS-CoV-2 antibodies with blocking buffer.

Table S6. The Hill equation derived for each of the drift-free curves when anti-RBD Ab is spiked in 1% human plasma. The final equation incorporates a multiplication factor of 100 to account for the dilution to determine the concentration anti-RBD Ab in the undiluted clinical specimen.

Row	**Max (mg/dL)**	**EC_{50} (ng/mL)**	**Equation**
A	333 ± 10	492 ± 52	x = 100(492/[(333/y)-1])
B	350 ± 10	519 ± 51	x = 100(519/[(350/y)-1])
C	360 ± 10	507 ± 52	x = 100(507/[(360/y)-1])
D	377 ± 11	470 ± 49	x = 100(470/[(377/y)-1])
E	375 ± 11	427 ± 47	x = 100(427/[(375/y)-1])
F	387 ± 10	400 ± 40	x = 100(400/[(387/y)-1])
G	402 ± 12	386 ± 43	x = 100(386/[(402/y)-1])
H	407 ± 11	359 ± 38	x = 100(359/[(407/y)-1])

Table S7. The Hill equation derived for each of the drift-free curves when anti-RBD Ab is spiked in 20% human plasma. The final equation incorporates a multiplication factor of 5 to account for the dilution to determine the concentration anti-RBD Ab in the undiluted clinical specimen.

Row	**Max (mg/dL)**	**EC_{50} (ng/mL)**	**Equation**
A	325 ± 9	580 ± 58	x = 5(580/[(325/y)-1])
B	342 ± 11	572 ± 63	x = 5(572/[(342/y)-1])
C	349 ± 11	576 ± 63	x = 5(576/[(349/y)-1])
D	368 ± 16	562 ± 83	x = 5(562/[(368/y)-1])
E	369 ± 17	470 ± 77	x = 5(470/[(369/y)-1])
F	385 ± 15	426 ± 60	x = 5(426/[(385/y)-1])
G	391 ± 12	411 ± 46	x = 5(411/[(391/y)-1])
H	403 ± 12	398 ± 44	x = 5(398/[(403/y)-1])

Table S8. The Hill equation derived for each of the drift-free curves when anti-Spike Ab is spiked in 20% human plasma. The final equation incorporates a multiplication factor of 5 to account for the dilution to determine the concentration anti-Spike Ab in the undiluted clinical specimen.

Row	**Max (mg/dL)**	**EC_{50} (ng/mL)**	**Equation**
A	441 ± 9	980 ± 59	x = 5(980/[(441/y)-1])
B	462 ± 9	967 ± 60	x = 5(967/[(462/y)-1])
C	463 ± 11	922 ± 65	x = 5(922/[(463/y)-1])
D	491 ± 9	932 ± 50	x = 5(932/[(491/y)-1])
E	487 ± 11	796 ± 59	x = 5(796/[(487/y)-1])
F	479 ± 12	701 ± 59	x = 5(701/[(701/y)-1])
G	500 ± 10	726 ± 46	x = 5(726/[(500/y)-1])
H	514 ± 11	687 ± 49	x = 5(687/[(514/y)-1])

Table S9. Calculated anti-RBD Ab and anti-Spike Ab concentrations for convalescent plasma donors. Clinical specimens were deidentified for this study; therefore, PD = confirmed positive donor and ND = confirmed negative donor. Measurements were made in triplicate for each donor per assay (*value exceeded upper limit of detection).

Clinical Specimen ID	[Anti-RBD Ab] (ng/mL)		[Anti-spike Ab] (ng/mL)	
	Mean	SE	Mean	SE
PD 1	2501	144	21332	28
PD 2	3505	97	11550	210
PD 3	0	0	1170	34
PD 4	1195	104	3742	89
PD 5	2220	51	6557	40
PD 6	2151	85	6855	30
PD 7	10427	574	12080	20
PD 8	4648	84	10763	236
PD 9	6955	59	11191	142
PD 10	1588	72	6684	59
PD 11	2888	31	8241	116
PD 12	16521	37	30909	90
PD 13	13439	45	26500	105
PD 14	10541	85	23742	93
PD 15	13633	33	37310	85
PD 16	16344	115	38248	59
PD 17	58957	95	*	*
PD 18	0	0	111	8
PD 19	0	0	3279	27
PD 20	381	25	1368	41
PD21	1663	23	6181	245
PD22	972	36	7037	78
PD23	1535	47	12807	101
PD24	4036	31	19674	75
PD25	787	82	4367	87

Table S9 (continued). Calculated anti-RBD Ab and anti-Spike Ab concentrations for convalescent plasma donors. Clinical specimens were deidentified for this study; therefore, PD = confirmed positive donor and ND = confirmed negative donor. Measurements were made in triplicate for each donor per assay (*value exceeded upper limit of detection).

Clinical Specimen ID	[Anti-RBD Ab] (ng/mL)		[Anti-spike Ab] (ng/mL)	
	Mean	SE	Mean	SE
PD26	1364	26	17326	65
PD27	2036	5	9521	107
PD28	2726	52	15468	34
PD29	2244	73	13791	38
PD30	3777	14	25580	104
PD31	1723	39	9347	78
PD32	2050	27	14784	94
PD33	2009	25	13987	135
PD34	903	8	5836	33
PD35	1388	6	14268	76
PD36	1151	37	13948	49
ND 1	0	0	0	0
ND 2	0	0	0	0
ND 3	0	0	0	0
ND 4	0	0	0	0

Table S10. Anti-RBD Ab Titration Concentrations for Plates with HRP anti-Human IgG pAb as the detection antibody. The MW of anti-RBD Ab is 146,499.88 Da.

pg/mL	fM
15.625	2.3
31.25	4.6
62.5	9.2
125	18.3
250	36.6
500	73.2
1000	146.5
1500	219.7
2000	293.0
3000	439.5
4000	586.0

Table S11. Anti-RBD Ab titration concentrations for used for plates with LC15 as the detection antibody. The MW of anti-RBD Ab is 146,499.88 Da.

ng/mL	nM
1.95	0.3
3.91	0.6
7.81	1.1
15.625	2.3
31.25	4.6
62.5	9.2
125	18.3
250	36.6
500	73.2
1000	146.5
1500	219.7
2000	293.0
3000	439.5
4000	586.0
5000	732.5

Table S12. Anti-spike Ab titration concentrations for used for plates with LC15 as the detection antibody. Anti-spike Ab is 1:1:1 mixture of commercially produced RBD (Abcam PN: ab273073), S1 (Novus Biologicals PN: NBP3-07956), and NTD (ACROBiosystems PN: SPD-S164) monoclonal antibodies. We were unable to convert the concentration from ng/mL to nM as the MW of the latter two antibodies were not disclosed by the manufacturers.

ng/mL
1.95
3.91
7.81
15.625
31.25
62.5
125
250
500
1000
1500
2000
3000
4000
5000

REFERENCES

(1) https://www.thermofisher.com/us/en/home/life-science/protein-biology/protein-assays-analysis/elisa/elisa-microplates-plasticware/guide-microplate-formats-well-designs.